Contribution from the Departments of Chemistry, Princeton University, Princeton, New Jersey 08544, and Rider College, Lawrenceville, New Jersey 08648

Resonance Raman Spectra and Excitation Profile for $[Fe_2O(O_2CCH_3)_2(HB(pz)_3)_2]$, a Hemerythrin Analogue

Roman S. Czernuszewicz,† John E. Sheats,‡ and Thomas G. Spiro*†

Received November 3, 1986

Resonance Raman (RR) spectra of the μ-oxo-bridged binuclear iron(III) center in the hemerythrin model complex $[Fe_2O(O_2CCH_3)_2(HB(pz)_3)_2]$ ($HB(pz)_3$ = hydrotris(1-pyrazolyl)borate anion; Armstrong W. H.; et al. *J. Am. Chem. Soc.* **1984**, *106*, 3653) have been investigated with variable-wavelength excitation and at low temperatures. The 530-cm^{-1} symmetric Fe–O–Fe stretch, ν_s, gives a strong excitation profile maximum at ~405 nm and a weaker one at ~525 nm. These two maxima are assigned to charge-transfer transitions to Fe^{III} from the two π orbitals of the bridging oxide ligand (energy separation ~5500 cm^{-1}). The two transitions are obscured in the complex electronic absorption spectra of the molecule. Low-temperature RR spectra with 406.7-nm excitation show a rich array of features, including the asymmetric Fe–O–Fe stretch, ν_{as} ($\Delta(^{16}O-^{18}O)$ = 35 cm^{-1}) at 754 cm^{-1}, a long progression of $n\nu_s$ overtones ($n \rightarrow 5$), and a subsidiary progression in $n\nu_s + 2\nu_{as}$ ($n \rightarrow 2$). The first overtone of ν_{as} is substantially stronger than the fundamental, reflecting the symmetry forbiddenness (B_2) of the latter. A plot of $\nu_s(n)/n$ vs. vibrational quantum number (n) yields a harmonic frequency, ω_s, of 532.5 ± 0.6 cm^{-1} (515.7 ± 0.7 cm^{-1}, ^{18}O) and an anharmonicity constant, X_{11}, of −1.23 ± 0.05 cm^{-1} (−1.25 ± 0.05 cm^{-1}, ^{18}O). A number of low-frequency bands have been assigned to Fe–N(pyrazole), Fe–O(acetate) stretching and angle deformation modes via a normal-coordinate analysis with a general valence force field. A relatively prominent 275-cm^{-1} band, shifting to 272 cm^{-1} upon ^{18}O substitution, is assigned to the stretching mode of the Fe–N(pyrazole) bond trans to the Fe–O bridge bond, the ^{18}O sensitivity being due to mixing with ν_s. The Fe–O–Fe angle deformation mode, δ, is reassigned to a band at 104 cm^{-1}. This mode forms a combination band at 633 cm^{-1} with ν_s ($\nu_s + \delta$ = 634 cm^{-1}) and also a difference band at 428 cm^{-1} ($\nu_s - \delta$ = 426 cm^{-1}). Identification of the latter band is confirmed via its ^{18}O shift and also by showing that it cools out at low temperatures. This is the first confirmed assignment of a resonance Raman difference band.

Introduction

There is much current interest in binuclear iron sites in proteins.[1] The best characterized example is the oxygen-carrying protein hemerythrin, for which high-resolution crystal structures are available for the metazido and metazidomyo forms.[2] A binuclear site is also present in ribonucleotide reductase[3] and possibly in uteroferrin.[4] Resonance Raman (RR) spectroscopy has provided important information about these protein sites via the vibrational modes of the Fe^{III}–O–Fe^{III} complex found in the oxidized or oxygenated forms.[5] It has recently become possible to study the properties of accurate models for these protein sites through the synthetic work of Armstrong et al.[6] and of Wieghardt et al.[7] Compounds have been prepared with an Fe^{III}–O–Fe^{III} unit and bridging carboxylate groups (acetate or propionate) that mimic the bridging glutamate and aspartate of hemerythrin. The compounds made by Armstrong et al. have hydrotris(1-pyrazolyl)borate ($HB(pz)_3^-$) ligands (see Figure 1) in place of the histidine ligands of hemerythrin, while those prepared by Wieghardt et al. contain instead the saturated amine 1,4,7-triazacyclononane (TACN) ligands. Resonance Raman spectra of these molecules[6,8] yield useful information about the nature of the molecular vibrations and their coupling to the excited states and provide reference points for protein data. In this work we provide a more complete analysis of the pyrazolylborate complex RR spectra. The excitation profile for the Fe–O–Fe symmetric stretching mode is reported, from which assignments for the O → Fe charge-transfer electronic transitions can be inferred.

Experimental Procedures

The $[Fe_2O(O_2CCH_3)_2(HB(pz)_3)_2]$ complex (**1**) was prepared as described in the literature.[6] ^{18}O exchange at the bridging position in **1** was accomlished by following the method described by Armstrong et al.,[6] except that the mixture of **1** (50 mg) and $H_2{}^{18}O$ (50 μL) in a small volume of CH_2Cl_2 was allowed to stir for only 2 h. The solvent was then removed in vacuo, and the resulting solid was used without further purification. Its Raman spectrum showed essentially 100% ^{18}O substitution at the μ-oxo position. Two weeks later, however, the same solid gave a spectrum showing a 40/60 mixture of ^{18}O and ^{16}O species. This result demonstrated that water from air readily exchanges its oxygen with the μ-oxo atom of **1** not only in the CH_2Cl_2 solution as previously reported by Armstrong et al.[6] but also in the crystalline state.

Electronic spectra of **1** in CH_2Cl_2 were recorded with a Cary Model 118 spectrometer. Exciting radiation for Raman spectra was provided by Coherent Radiation Model CR-5 Ar^+ (457.9–514.5 nm) and Spectra Physics Model 171 Kr^+ (337.4–647.1 nm) ion lasers. The scattered radiation was dispersed by a Spex 1401 double monochromator and detected by a cooled RCA 31034A photomultiplier using an ORTEC 9315 photon counter. The data were collected digitally with a DEC MINC2 computer. All RR spectra were measured with the sample dispersed in KCl pellets. The experimental technique used for the low-temperature solid spectra (77 K) has been described elsewhere.[9] RR spectra at variable temperatures (10–298 K) were measured on a KCl pellet attached to a cold station of Air Products Model DE 202 closed-cycle liquid-He refrigerator. The relative intensity of the 530-cm^{-1} band plotted in the excitation profile was measured against the 985-cm^{-1} band

* To whom correspondence should be addressed.
† Princeton University.
‡ Rider College.

(1) (a) Lippard, S. J. *Chem. Br.* **1986**, *22*, 222–229. (b) Wilkins, R. G.; Harrington, *Adv.Inorg. Biochem.* **1983**, *5*, 51–85. (c) Sanders-Loehr, J.; Loehr, T. M. *Adv. Inorg. Biochem.* **1979**, *1*, 235–252. (d) Stenkamp, R. E.; Jensen, L. H. *Adv. Inorg. Biochem.* **1979**, *1*, 219–233. (e) Kurtz, D. M., Jr.; Shriver, D.; Klotz, I. M. *Coord. Chem. Rev.* **1977**, *24*, 145–178. (f) Okamura, M. Y.; Klotz, I. M. In *Inorganic Biochemistry*; Eichhorn, G. L., Ed.; Elsevier: Amsterdam, 1973; p 320.
(2) (a) Hendrickson, W. A. In *Invertebrate Oxygen-Binding Proteins: Structure, Active Site, and Function*; Lamy, J., Lamy, J., Eds.; Marcel-Dekker: New York, 1981; pp 503–515. (b) Stenkamp, R. E.; Sieker, L. C.; Jensen, L. M.; Sanders-Loeher, J. *Nature (London)* **1981**, *291*, 263–264. (c) Stenkamp, R. E.; Sieker, L. C.; Jensen, L. H. *J. Am. Chem. Soc.* **1984**, *106*, 618–622.
(3) (a) Thelander, L.; Reichard, P. *Annu. Rev. Biochem.* **1979**, *48*, 133–158. (b) Reichard, P.; Ehrenberg, A. *Science (Washington, D.C.)* **1983**, *221*, 514–519. (c) Sjöberg, B.-M.; Gräslund, A. *Adv. Inorg. Biochem.* **1983**, *5*, 87–110.
(4) Anatanaitis, B. C.; Aisen, P. *Adv. Inorg. Biochem.* **1983**, *5*, 111–136.
(5) (a) Dunn, J. B. R.; Shriver, D. F.; Klotz, I. M. *Proc. Natl. Acad. Sci. U.S.A.* **1973**, *70*, 2582–2584. (b) Dunn, J. B. R.; Adison, A. W.; Bruce, R. E.; Sanders-Loehr, J.; Loehr, T. M. *Biochemistry* **1977**, *16*, 1743–1479. (c) Freier, S. M.; Duff, L. L.; Shriver, D. F.; Klotz, I. M. *Arch. Biochem. Biophys.* **1980**, *205*, 449–463. (d) Solbrig, R. M.; Duff, L. L.; Shriver, D. F.; Klotz, I. M. *J. Inorg. Biochem.* **1982**, *17*, 69–74. (e) Sjöberg, B.-M.; Loehr, T. M.; Sanders-Loehr, J. *Biochemistry* **1982**, *21*, 96–101. (f) Shiemke, A. K.; Loehr, T. M.; Sanders-Loehr, J. *J. Am. Chem. Soc.* **1984**, *106*, 4951–4956.
(6) Armstrong, W. H.; Spool, A.; Papaefthymiou, G. C.; Frankel, R. B.; Lippard, S. J. *J. Am. Chem. Soc.* **1984**, *106*, 3653–3667.
(7) Wieghardt, K.; Pohl, K.; Gebert, W. *Angew. Chem., Int. Ed. Engl.* **1983**, *22*, 727.
(8) Spool, A.; Williams, I. D.; Lippard, S. J. *Inorg. Chem.* **1985**, *24*, 2156–2162.
(9) Czernuszewicz, R. S.; Johnson, M. K. *Appl. Spectrosc.* **1983**, *37*, 297–298.

0020-1669/87/1326-2063$01.50/0 © 1987 American Chemical Society

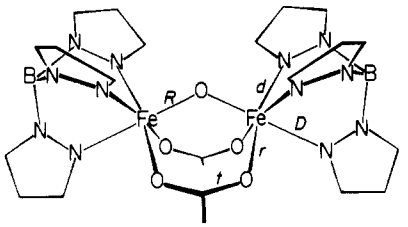

Figure 1. Structure and internal coordinates of the $[Fe_2O(O_2CCH_3)_2(HB(pz)_3)_2]$ complex.

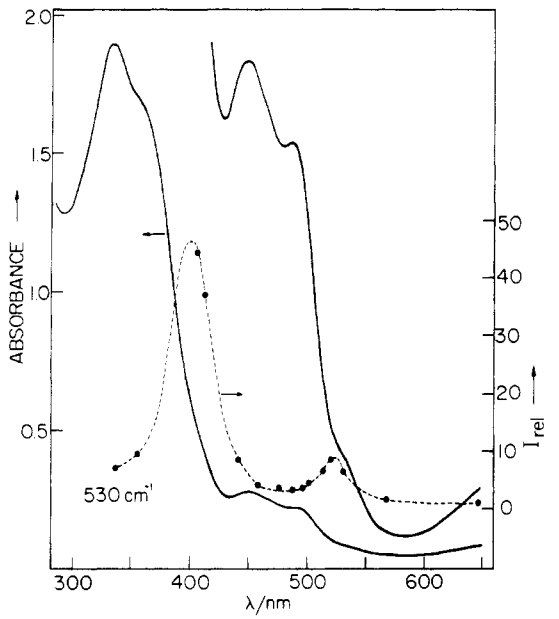

Figure 2. Relative Raman intensity (I_{rel}) profile for the ν_s(Fe–O–Fe) stretching mode at 530 cm^{-1} of $[Fe_2O(O_2CCH_3)_2(HB(pz)_3)_2]$, superimposed on the electronic spectrum. Raman band intensities were determined relative to the 985-cm^{-1} $\nu_1(SO_4^{2-})$ band and normalized to the intensity at the 6471-Å excitation wavelength.

of the internal standard, K_2SO_4, which was mixed homogeneously with the sample in a KCl pellet. For these data the KCl pellet was rotated, under a N_2 atmosphere,[10] to avoid thermal decomposition. All intensities plotted were corrected for the ν^4 dependence[11] and normalized to the intensity obtained at 647.1 nm. Normal-mode calculations were performed by using the **GF** matrix method[12] and a generalized valence force field. Schachschneider's programs[13] were used for constructing **G** matrices and solving the secular equations.

Results and Discussion

A. Excitation Profile. The strongest band in the RR spectra of $[Fe_2O(O_2CCH_3)_2(HB(pz)_3)_2]$ (**1**) is the 530-cm^{-1} symmetric Fe–O–Fe stretch, which shifts to 513 cm^{-1} when ^{18}O is substituted in the bridge.[6] Figure 2 compares the excitation profile (EP) for this band, measured relative to the 985-cm^{-1} ν_1 band of SO_4^{2-} present as an internal standard, with the absorption spectrum. Two well-defined maxima are seen in the EP, at ~405 and ~525 nm. The latter was also observed by Armstrong et al.[6] for solution spectra, but only one point at 363.8 nm was available at wavelengths lower than 457.9 nm; the intensity at this near-UV wavelength was found to be ~100-fold higher than in the visible region. Our 356.5-nm intensity, however, is down in the range of the visible excitation intensities, whereas the 406.7-nm and 413.1-nm points are much higher. Medium effects may be responsible for the altered relative intensities.

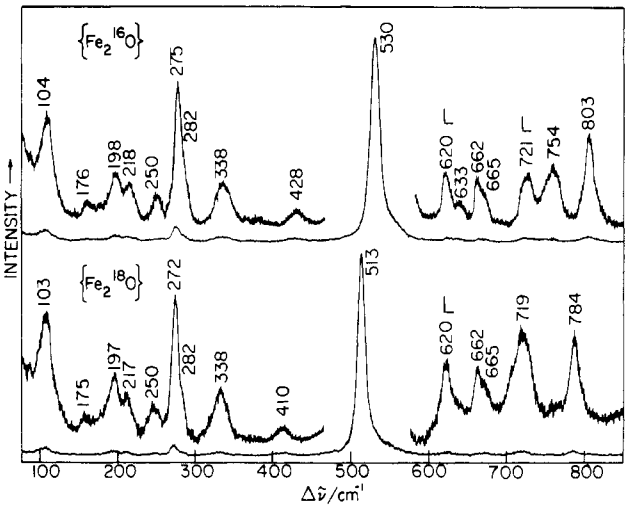

Figure 3. Low-temperature (77 K) resonance Raman spectra of crystalline $[Fe_2O(O_2CCH_3)_2(HB(pz)_3)_2]$ and its μ-^{18}O analogue obtained with 4067-Å excitation (100 mW) and 5-cm^{-1} slit width. "L" marks bands associated with internal modes of $HB(pz)_3^-$ ligands.

It is expected that the Fe–O–Fe stretching mode couples effectively to O → Fe charge-transfer (CT) transitions, and it is likely that the two excitation profile maxima result from such transitions. Several CT transitions are possible, there being three potential donor orbitals on O^{2-} and five potential acceptor orbitals on Fe^{III}. The latter are divided into two groups, d_π and d_σ, with an energy separation, $10Dq \approx 10000$ cm^{-1} for high-spin Fe^{III}.[14,15] The separation between the two EP maxima, ~5500 cm^{-1}, is much less than this. We tentatively assign these bands to transitions from different O^{2-} orbitals to the Fe d_π orbital set. Since the O^{2-} σ orbital is low in energy, due to the bonding interaction with Fe, the donor orbitals for the visible–near-UV CT transitions are suggested to be the two π orbitals, oriented in and out of the Fe–O–Fe plane for the higher and lower transitions, respectively.

The EP maxima correspond to relatively weak shoulders in the electronic spectrum, which contain several absorption bands. These may arise from other charge-transfer transitions, as well as ligand field and simultaneous pair excitations whose intensities are augmented by the spin coupling in the Fe–O–Fe system.[15] A similar conclusion has been reached from an analysis of the hemerythrin derivatives and Fe–O–Fe model compounds.[16] The excitation profile offers a dramatic instance of the ability of RR enhancement to pick out specific electronic transitions in a complex absorption spectrum.

The O → Fe charge-transfer energies are expected to be sensitive to the Fe–O–Fe bridging angle and to the orientation and energies of the Fe d orbitals, as determined by the capping ligands. The EP of the Fe–O–Fe stretch in oxyhemerythrin shows a maximum at ~375 nm, close to that seen for the higher energy peak of Figure 2, but no enhancement is seen in the 520-nm region.[5f] Apparently, the lower energy CT transition is less effective in oxyhemerythrin; the altered d-orbital orientations associated with the presence of five imidazole ligands and an O_2 ligand in the protein vs. six pyrazolyl ligands in the model may be involved. On the other hand, azidomethemerythrin shows two visible EP maxima,[5] at ~430 and ~525 nm; the intensity is rising at 350 nm, presumably toward another maximum, at somewhat higher energy than seen in the present case or in oxyhemerythrin. The two visible-region EP maxima suggest a splitting of the lower energy O → Fe transition, due to the electronic properties of the azide ligand. Two visible-region EP maxima, at ~480 and ~520 nm have also been reported[8] for Wieghardt's compound, again

(10) Czernuszewicz, R. S. *Appl. Spectrosc.* **1986**, *40*, 571–573.
(11) Spiro, T. G.; Stein, P. *Annu. Rev. Phys. Chem.* **1977**, *28*, 501–521.
(12) Wilson, E. B.; Decius, J. C.; Cross, P. C. *Molecular Vibrations*; McGraw-Hill: New York, 1955.
(13) Schachtschneider, J. H. Technical Report No. 263–62; Shell Development Co.: Emeryville, CA, 1962.
(14) Hush, N. S.; Hobbs, R. J. M. *Prog. Inorg. Chem.* **1968**, *10*, 259–359.
(15) Schugar, H. J.; Rossman, G. R.; Barraclough, C. G.; Gray, H. B. *J. Am. Chem. Soc.* **1972**, *94*, 2683–2690.
(16) Wheeler, W. D.; Shiemke, A. K.; Averill, B. A.; Loehr, T. M.; Sanders-Loehr, J., private communication.

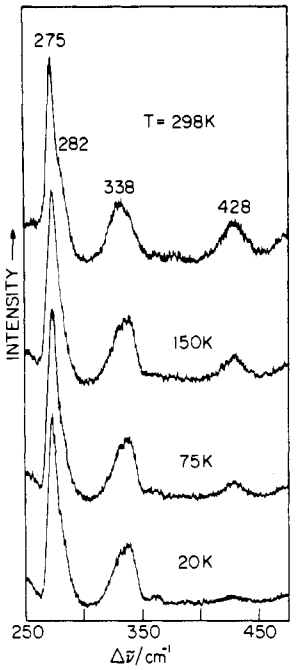

Figure 4. Intensity temperature dependence of the 428-cm^{-1} ν_s(Fe–O–Fe) – δ(Fe–O–Fe) difference Raman band for $[Fe_2O(O_2CCH_3)_2(HB(pz)_3)_2]$. All spectra were obtained with 4067-Å excitation from a KCl pellet attached to a liquid-He closed-cycle refrigerator cold finger.[10]

suggesting a splitting of the CT transition. Although the systematics have yet to be worked out, it is evident that the EP's are sensitive to the details of the electronic structure at the binuclear iron center.

B. Normal-Mode Calculations and Assignments. Figure 3 shows the 406.7-nm excited RR spectrum of polycrystalline **1** in a KCl pellet obtained at low temperature (~77 K). Because of the strong enhancement at this wavelength, and the low temperature, there is much more detail than in spectra obtained previously with longer wavelength excitation on room-temperature CH_2Cl_2 solution and neat solid samples.[6] The 530- and 275-cm^{-1} bands and a shoulder at 282 cm^{-1} were reported previously[6] at somewhat lower frequencies in the room-temperature solid spectrum (528, 269, and 278 cm^{-1}, respectively). The 278-cm^{-1} shoulder was reported[6] to move under the 269-cm^{-1} band in the ^{18}O derivative and was identified with the Fe–O–Fe angle deformation mode.[6] In the low-temperature spectrum (Figure 3) the 282-cm^{-1} shoulder is not affected by ^{18}O substitution, but a small ^{18}O isotope shift (~3 cm^{-1}) is observed for the main 275-cm^{-1} band.

Also observed in Figure 3 is a band at 754 cm^{-1}, shifting to 719 cm^{-1} after ^{18}O exchange, which had been identified in the IR ^{16}O–^{18}O difference spectrum[6] as the asymmetric Fe–O–Fe stretch. This mode is of B_2 symmetry in the C_{2v} point group of the molecule and requires a vibronic (*B* term) mechanism[11] for activation in the RR spectrum in contrast to the 530-cm^{-1} totally symmetric stretch, which is Franck–Condon (*A* term) allowed. The 754/530 cm^{-1} intensity ratio is only 0.08 at 406.7 nm. Also reported previously[6] was the ^{18}O-sensitive 803-cm^{-1} band, identified as a combination band, 530 plus 275 cm^{-1} (19-cm^{-1} ^{18}O shift vs. 20 cm^{-1} expected).

Two other, previously unrecognized, ^{18}O-sensitive bands are seen weakly in Figure 3, at 633 and 428 cm^{-1}. The 633-cm^{-1} band shifts under the nearby 620-cm^{-1} band in the ^{18}O spectrum, while the 428-cm^{-1} band shifts down to 410 cm^{-1}. This shift is essentially the same as that seen for the 530-cm^{-1} Fe–O–Fe symmetric stretch. The 633- and 428-cm^{-1} bands are assigned to sum and difference combinations between the 530-cm^{-1} band and a band seen at 104 cm^{-1}. If the 428-cm^{-1} band is due to a difference mode, then its intensity should diminish as the temperature is lowered and the initial level (104 cm^{-1}) is depopulated. Figure 4 shows that this does indeed happen; as the temperature is lowered, the 428-cm^{-1} band steadily loses intensity relative to its 338- and 275-cm^{-1} neighbors. This is the first positive identification of a RR difference band, although the possibility that such bands might be resonance enhanced has earlier been suggested.[17]

Several other bands (<250 cm^{-1}) are seen that shift by no more than 1 cm^{-1} upon ^{18}O substitution. They were tentatively identified with the aid of a normal-mode analysis, based on an approximate model in which the pyrazolylborate ligands were replaced by three

Table I. Bond Distances (Å) and Angles (deg) in $[Fe_2O(O_2CCH_3)_2(HB(pz)_3)_2]$[a]

bond dist		angle	
$R(\mu$-O–Fe)	1.784	∠(*R*,*R*)	123.6
r(Fe–OAc)	2.042	∠(*R*,*r*)	96.5
D(Fe–N_{trans})	2.188	∠(*r*,*r*)	90.8
d(Fe–N_{cis})	2.152	∠(*R*,*D*)	177.4
t(C–O)	1.256	∠(*d*,*d*)	84.6
		∠(*D*,*d*)	82.4
		∠(*t*,*t*)	125.6

[a] Taken from ref 6.

Table II. Force Constants (mdyn/Å) for $[Fe_2O(O_2CCH_3)_2(HB(pz)_3)_2]$[a]

K(C–O)	11.20	*H*(OAc–Fe–OAc)	0.40
K(Fe–O)	3.00	*H*(OAc–Fe–N_{cis})	0.20
K(Fe–N_{trans})	1.45[b]	*H*(OAc–Fe–N_{trans})	0.20
K(Fe–N_{cis})	1.50[b]	*H*(N_{cis}–Fe–N_{cis})	0.10
K(Fe–OAc)	1.20	*H*(N_{cis}–Fe–N_{trans})	0.10
H(O–C–O)	1.80	*H*(Fe–O–Ac)	0.10
H(Fe–O–Fe)	0.27	*k*(Fe–O/Fe–O)	0.10
H(O–Fe–N_{cis})	0.10	*k*(Fe–O/Fe–N_{trans})	0.15
H(O–Fe–OAc)	0.10	*k*(Fe–OAc/Fe–N_{cis})	0.25

[a] *K* = stretching force constant; *H* = bending force constant; *k* = stretch–stretch interaction force constant. [b] *K*(Fe–N) force constants were scaled according to Badger's rule (Badger, R. M. *J. Chem. Phys.* **1936**, *2*, 128).

Table III. Calculated and Observed Raman Frequencies (cm^{-1}) and Their Assignment for $[Fe_2(O_2CCH_3)_2(HB(pz)_3)_2]$

C_{2v} mode symm	calcd[a]	obsd[a]	assignt[b]
		Predominantly ν(Fe–O–Fe)	
B_2	754 (35.6)	754 (35)	ν_{as}(Fe–O–Fe) (98)
A_1	529 (17.1)	530 (17)	ν_s(Fe–O–Fe) (81) + ν(Fe–N_{trans}) (7) + δ(Fe–O–Fe) (6)
		Predominantly δ(O–C–O)	
A_1	661	662	δ(O–C–O) (87)
B_1	663	665	δ(O–C–O) (81)
		Predominantly ν(Fe–OAc)	
A_2	440		ν(Fe–OAc) (68) + ν(Fe–N_{cis}) (22)
B_1	394		ν(Fe–OAc) (45) + ν(Fe–N_{cis}) (38)
B_2	365	360[c]	ν(Fe–OAc) (55) + ν(Fe–N_{cis}) (36)
A_1	341	338	ν(Fe–OAc) (45) + ν(Fe–N_{cis}) (41)
		Predominantly ν(Fe–N_{pz})	
B_2	284	282	ν(Fe–N_{cis}) (64)
A_1	272 (4.6)	275 (3)	ν(Fe–N_{trans}) (77) + δ(Fe–O–Fe) (12) + ν_s(Fe–O–Fe) (5)
B_2	274 (2)		ν(Fe–N_{trans}) (78)
A_1	244	250	ν(Fe–N_{cis}) (51) + ν(Fe–OAc) (41)
A_2	237	218 (1)	ν(Fe–N_{cis}) (60) + ν(Fe–OAc) (27)
B_1	202 (1)	198 (2)	ν(Fe–N_{cis}) (50) + ν(Fe–OAc) (43)
		Cluster Angle Deformation	
A_1	107 (1)	104 (1)	δ(Fe–O–Fe) (39) + δ(O–Fe–OAc) (19) + ν(Fe–N_{trans}) (12)

[a] ν = stretching mode, δ = bending mode; parentheses indicate calculated or observed μ-$^{18}O \rightarrow \mu$-^{16}O isotopic shifts. [b] Numbers in parentheses indicate potential energy distribution, %. [c] Seen with 5145-Å excitation.

(17) Friedman, J. M.; Hochstrasser, R. M. *Chem. Phys.* **1973**, *1*, 457–467.

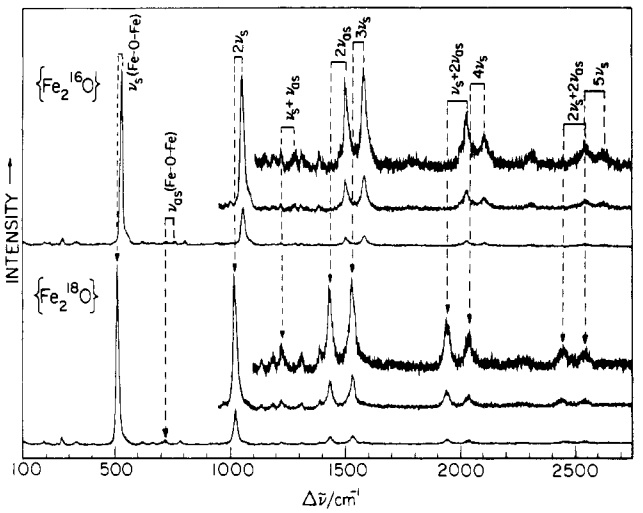

Figure 5. Low-temperature Fe–O–Fe overtone region resonance Raman spectra of crystalline $[Fe_2O(O_2CCH_3)_2(HB(pz)_3)_2]$ and its μ-^{18}O analogue obtained with 4067-Å excitation (150 mW) and 7-cm^{-1} slit width.

point masses each, at the position of the ligated N atoms. The masses were chosen to be 64, the full mass of the pyrazolyl ring, which is expected to move as a rigid body in the Fe–N stretching modes, consonant with results obtained previously for pyridine[18] and imidazole ligands.[19] All of the remaining atoms of the molecule were included, except that the acetate CCH_3 groups were replaced by mass 27 atoms. Structural parameters, which are listed in Table I, were taken from the crystal structure established by Armstrong et al.[6] A general valence force field was used, and the force constants were adjusted to reproduce the observed frequencies and isotope shifts. The final set of force constants is given in Table II. Table III gives calculated frequencies and potential energy distributions for those modes involving Fe–O or Fe–N stretching, primarily, and deformation modes of the $Fe_2O(O_2CCH_3)_2$ bridge.

The Fe–O–Fe modes, and isotope shifts, are calculated correctly, with force constants that are in good agreement with those used in previous simplified three-body calculations.[6,8]

The ^{18}O sensitivity of the 275-cm^{-1} band can be explained if the mode is associated primarily with the stretching of Fe–pyrazole bonds trans to the Fe–O bridge bonds, coupling between these coordinates being maximal for a N–Fe–O angle of 180°. Indeed, the predicted isotope shift for a 272-cm^{-1} band consisting primarily of $Fe–N(pyrazole)_{trans}$ is ~5 cm^{-1}. The second Fe–N trans mode with B_2 symmetry is predicted to lie close by (274 cm^{-1}) with a smaller (2 cm^{-1}) ^{18}O isotope shift due to coupling with the higher lying asymmetric Fe–O–Fe stretch. Although the observed isotope shift, 3 cm^{-1}, is consistent with either assignment, it seems reasonable that the A_1 mode should be more intense, especially since it couples with the very strong 530-cm^{-1} Fe–O–Fe symmetric stretch. A RR band of hemerythrin at 292 cm^{-1} was originally assigned to Fe–imidazole stretching[5b,c] but was reassigned to Fe–O–Fe bending on the basis of a 6-cm^{-1} ^{18}O shift. We believe the original assignment to be correct and that the ^{18}O shift is due to coupling between Fe–O and trans Fe–N(histidine) bonds.

The assignment of a Fe–O–Fe bending mode is not particularly meaningful, since this coordinate mixes into several of the low-frequency deformation modes of the $Fe_2O(O_2CCH_3)_2$ bridging system. As indicated in Table III, the 107-cm^{-1} calculated mode has the largest δ(Fe–O–Fe) contribution, 39%, and we assign it to the fairly prominent band at 104 cm^{-1}. This band is calculated, and observed, to undergo only a 1-cm^{-1} ^{18}O shift, reflecting the small contribution of the relatively light O atom to the eigenvector (which involves motion of the Fe atoms primarily). This is the mode that forms both sum and difference bands with the 530-cm^{-1} Fe–O–Fe symmetric stretch.

Table IV. Observed Overtone and Combination Wavenumbers in the RR Spectrum of $[Fe_2O(OAc)_2(HB(pz)_3)_2]$ (4067-Å Excitation)

band[a]	cm^{-1} ^{16}O	cm^{-1} ^{18}O	band[a]	cm^{-1} ^{16}O	cm^{-1} ^{18}O
$n\nu_s$(Fe–O–Fe) Progression					
ν_s	530	513	$4\nu_s$	2105	2036
$2\nu_s$	1058	1024	$5\nu_s$	2627	2539
$3\nu_s$	1583	1532			
$n\nu_s$(Fe–O–Fe) + $2\nu_{as}$(Fe–O–Fe) Progression					
$\nu_s + 2\nu_{as}$	2028	1941	$2\nu_s + 2\nu_{as}$	2550	2444
Other Overtone and Combination Modes					
$\nu_s - \delta$(Fe–O–Fe)	428	410	$\nu_s + \nu_{as}$	1284	1230
$\nu_s + \delta$(Fe–O–Fe)	633	620[b]	$2\nu_{as}$	1504	1432
$\nu_s + \nu(Fe–N_{trans})$	803	784			

[a] ν_s and ν_{as} = symmetric and asymmetric stretching modes, respectively; δ = bending mode. [b] Overlapped with ligand mode.

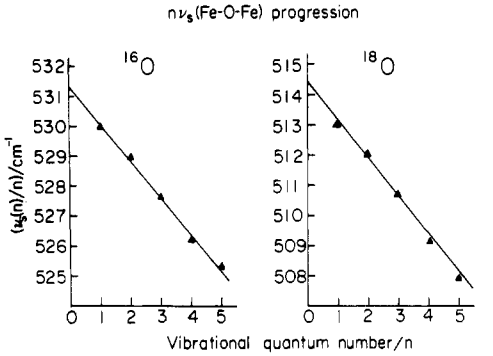

Figure 6. Plots of $\nu(n)/n$ vs. n for $n\nu_s$(Fe–O–Fe) progressions for $[Fe_2O(O_2CCH_3)_2(HB(pz)_3)_2]$ and its μ-^{18}O analogue.

In addition to the trans Fe–N(pyrazole) stretches discussed above, four modes associated primarily with the stretching of cis Fe–N(pyrazole) bonds are expected in the ~250-cm^{-1} region. These are calculated at frequencies from 202 to 284 cm^{-1} and find counterparts with observed bands in the RR spectrum. In addition, four Fe–O(acetate) stretching modes are anticipated in the ~400-cm^{-1} region, although the lower two frequencies (A_1 and B_2) have heavy admixtures from Fe–N(pyrazole) stretching. Candidates for these two modes are seen in the RR spectrum. Finally, two bands are seen, at 665 and 662 cm^{-1}, which are calculated to arise from modes that involve deformation of the O–C–O acetate angles primarily.

C. Overtone and Combination Spectra. Figure 5 is a scan of 406.7-nm excited RR spectra out to 2700 cm^{-1}. A striking series of overtones of the Fe–O–Fe symmetric stretch, ν_s, can be seen, out to $5\nu_s$. Another intriguing observation is that the first overtone of the asymmetric Fe–O–Fe stretch, ν_{as}, is stronger than the fundamental. Overtone/fundamental intensity ratios are generally $\ll 1$, but in this case, the fundamental is of B_2 symmetry and, as noted above, requires a vibronic mechanism (generally much weaker than a Franck–Condon mechanism) for activation, whereas its overtone is of $A_1(B_2XB_2)$ symmetry and is Franck–Condon-allowed. Not only does $2\nu_{as}$ show appreciable RR intensity (about equal to $3\nu_s$) but it forms a subsidiary progression with ν_s, out to $2\nu_s + 2\nu_{as}$. The combination of ν_s with the ν_{as} fundamental is also detectable. All of these features can readily be sorted out by their ^{18}O shifts (See Table IV).

Figure 6 shows that the $n\nu_s$ progression is well-behaved, a plot of frequency against vibrational quantum number being accurately linear for both ^{16}O and ^{18}O. These plots[20] provide harmonic frequencies, ω_s = 532.5 ± 0.6 cm^{-1} for ^{16}O and 515.7 ± 0.7 cm^{-1} for ^{18}O, and an anharmonicity constant, X_{11} = −1.25 ± 0.05 cm^{-1}, which is the same, within experimental error, for ^{16}O and ^{18}O.

(18) Wright, P. G.; Stein, P.; Burke, P. M.; Spiro, T. G. *J. Am. Chem. Soc.* **1979**, *101*, 3531–3535.
(19) Nestor, L.; Larrabee, J. A.; Woolery, G.; Reinhammar, B.; Spiro, T. G. *Biochemistry* **1984**, *23*, 1084–1093.
(20) Clark, R. J. H.; Stewart, B. *Struct. Bonding (Berlin)* **1979**, *36*, 1–81.

The X_{11}/ω_1 ratios, 2.32×10^{-3} for ^{16}O and 2.44×10^{-3} for ^{18}O, are in the range found for other metal–ligand stretching modes.[20]

Summary

RR scattering of **1** is dominated by the symmetric Fe–O–Fe stretching mode, ν_s, at 530 cm^{-1}, enhanced via coupling with O → Fe CT transitions. Its excitation profile reveals two CT transitions, at ~405 and ~525 nm, suggested to originate in the two O^{2-} p_π orbitals and terminate in the Fe^{III} d_π orbitals. When maximally enhanced, the ν_s mode supports detectable combination bands with modes at 275 and 104 cm^{-1}. The latter even forms a difference band with ν_s, which loses intensity at low temperature, as required. A progression in ν_s overtones out to $5\nu_s$ is observed, from which accurate harmonic frequency and anharmonicity constants are calculated. The asymmetric Fe–O–Fe stretch, ν_{as} = 754 cm^{-1}, is detectable but very weak; being of B_2 symmetry, it is enhanced only by vibronic mixing. Its overtone, being of A_1 symmetry, is Franck–Condon-allowed, has greater intensity, and also forms a subsidiary series with ν_s. Assignments of other low-frequency modes to Fe–N(pyrazole) and Fe–O(acetate) stretching and Fe–O–Fe and O–C–O(acetate) deformations are suggested on the basis of a normal-coordinate analysis. Of particularly interest are the assignments of moderately strong bands at 275 and 104 cm^{-1} to Fe–N(pyrazole) stretching and (mainly) Fe–O–Fe bending, respectively. The 3-cm^{-1} ^{18}O shift of the 275-cm^{-1} band is due to coupling between the Fe–N(pyrazole)$_{trans}$ and Fe–O_{bridge} bonds. By analogy, the ^{18}O-sensitive 292-cm^{-1} band of azidomethemerythrin is reassigned to the Fe–N(histidine)$_{trans}$ stretch.

Acknowledgment. Helpful discussions with Drs.J. Sanders-Loehr, S. J. Lippard, and H. B. Gray are gratefully acknowledged. This work was supported by NIH Grant GM13498.

Registry No. $Fe_2O(O_2CCH_3)_2(HB(pz)_3)_2$, 86177-70-0; ^{18}O, 14797-71-8.

Contribution from the Department of Chemistry, University of Pittsburgh, Pittsburgh, Pennsylvania 15260

Pentaammineruthenium(II/III) Imidazole and Imidazolate Complexes of 2-Carboxylatoimidazole and 2-Imidazolecarboxaldehyde

Michael G. Elliott and Rex E. Shepherd*

Received December 5, 1986

$(NH_3)_5RuL^{2+}$ and $(NH_3)_5RuL^{3+}$ complexes of 2-substituted imidazoles, L = 2-carboxylatoimidazole ($2CO_2imH^-$) and 2-imidazolecarboxaldehyde (2CHOimH), have been prepared and characterized by UV–visible spectroscopy, potentiometric titration, and differential-pulse voltammetry. An aldehyde carbonyl/hydrate equilibrium was detected for the free 2CHOimH ligand by ^1H NMR and UV–visible methods. Above pH ≅7 the R = CHO derivative is highly favored over the hydrate, R = $CH(OH)_2$ ($K \leq 7 \times 10^{-4}$ M^{-1} for hydration). Protonation at N3 of 2CHOimH induces hydration (K = 143 at pH 3.17). Thus 2CHOimH is less hydrated than 4-formylpyridine (pfp) by at least 2 orders of magnitude while $2CHOimH_2^+$ is more extensively hydrated than $Hpfp^+$ ($K \sim 3$) by 1 order of magnitude. Coordination of either $(NH_3)_5Ru^{2+}$ or $(NH_3)_5Ru^{3+}$ with $2CO_2imH^-$ or 2CHOimH enhances the acidity of the pyrrole hydrogen. Results determined in this work show that the effects of an organic ring substituent and the coordinated Ru center are virtually additive on stabilizing the imidazolato form ($Ru^{III} > Ru^{II}$; R = CHO > R = CO_2^-). pK_a's for the complexes are as follows (T = 22 °C): $(NH_3)_5Ru^{III}(2CO_2imH)^{2+}$, 7.95 ± 0.05; $(NH_3)_5Ru^{III}(2CH(OH)_2imH)^{3+}$, 5.65 ± 0.05; $(NH_3)_5Ru^{II}(2CHOimH)^{2+}$, ~8.8 compared to the free ligand pK_a's of 10.7 ($2CO_2imH^-$) and 10.5 (2CHOimH). $(NH_3)_5Ru^{II}L$ complexes exhibit two MLCT transitions that establish a π-acceptor order for 2-substituted imidazoles with R = CHO > CO_2^- ≫ H. These MLCT bands occur at 367 nm ($\epsilon = 2.0 \times 10^3$ M^{-1} cm^{-1}) and 420 nm ($\epsilon = 4.6 \times 10^3$ M^{-1} cm^{-1}) for $(NH_3)_5Ru^{II}(2CO_2imH)^+$ and 467 nm ($\epsilon = 4.6 \times 10^3$ M^{-1} cm^{-1}) and 583 nm ($\epsilon = 1.5 \times 10^3$ M^{-1} cm^{-1}) for $(NH_3)_5Ru^{II}$-$(2CHOimH)^{2+}$. These are attributed to $\pi^*_{ring} \leftarrow \pi d$ and $\pi^*_R \leftarrow \pi d$ transitions. The strong π-acceptor character of 2CHOimH (comparable in magnitude to pyrazine) is further established by the $E°$ for $(NH_3)_5Ru(2CHOimH)^{3+/2+}$ of 0.322 V. The LMCT bands ($\pi d \leftarrow (\pi_1)_L$ and $\pi d \leftarrow (\pi_{2,n})$) of the $(NH_3)_5Ru^{3+}$ complexes establishes the π-donor order of 2-substituted imidazoles of R = $CH(OH)_2 > CH_3 > H > CO_2^-$. $(NH_3)_5Ru^{III}(2CO_2im)^+$ dissociates by an I_d-type mechanism with k_d = (1.35 ± 0.03) × 10^{-4} s^{-1}; μ = 2.0 M NaCl, and T = 22 °C. Substitution of $2CO_2imH^-$ on $(NH_3)_5RuOH_2^{2+}$ is slower than substitution of imH; a steric rate reduction of ca. 240 times is implicated after correction for the 10-fold rate increase for anionic vs. neutral ligands. The influence of $(NH_3)_5Ru^{2+}$ and $(NH_3)_5Ru^{3+}$ on 2CHOimH as a ligand is similar to their influence on pfp; Ru^{III} strongly favors the hydration of either ligand while the substantial π-acceptor character of R = CHO favors the carbonyl form for Ru^{II}. The effect is particularly noteworthy for 2CHOimH because imidazoles are generally poor π-acceptors; incorporation of R = CHO introduces the capacity of the imidazole ring to stabilize soft metal centers via a π-acceptor role.

Introduction

Imidazole (Him) and the imidazolate ion (im^-) are of considerable interest in their role as ligands for transition-metal centers in small molecule coordination compounds or in active sites of metalloproteins and metalloenzymes. In the biopolymers the metal center attachment is produced through the amino acid residue histidine. The imidazole ligand appears in a wide variety of redox active and metabolic enzymes, particularly those with Cu(II), Zn(II), Mn(II), or Fe(II) active centers. The modified imidazole, benzimidazole, acts as an axial base in the dietary required vitamin B-12 unit, which contains Co(III). Polymer-supported N-heterocycles, including the pyridines and imidazoles, are being used as a means of supporting redox-active centers for chemical separations of costlier trace metals and as active surfaces for derivatized electrode purposes. For these reasons, the studies of the metal–imidazole interaction in terms of affinity properties and the manner in which the imidazole moiety will affect the redox properties and stabilities of the oxidation states of a given metal center impinges widely on the research areas of biochemistry, coordination chemistry, and homogeneous catalysis.

Recent research in our laboratory has revealed a rather striking range of kinetic, physical, and spectral influences of the imidazole or its imidazolate form on the chemistry of its complexes. For example, chemical shift patterns for the ^1H and ^{13}C NMR resonances in diamagnetic imidazole complexes such as the $(NH_3)_5Co^{III}L$ series show clear differences from those of the related pyridine derivatives.[1,2] The d^n configuration of the metal center exhibits a marked influence, greater than the ionic potential, on the pK_a of the pyrrole ring proton of imidazoles; the effect has

(1) Henderson, W. W.; Shepherd, R. E.; Abola, J. *Inorg. Chem.* **1986**, *25*, 3157–3163.
(2) Hoq, M. F.; Johnson, C. R.; Paden, S.; Shepherd, R. E. *Inorg. Chem.* **1983**, *22*, 2693–2700.

0020-1669/87/1326-2067$01.50/0 © 1987 American Chemical Society